doi:10.1006/jmbi.2001.5155 available online at http://www.idealibrary.com on IDEAL® *J. Mol. Biol.* (2001) **314**, 663–669

JMB

COMMUNICATION

Enhanced Crystallization of the Cys18 to Ser Mutant of Bovine γB Crystallin

Neer Asherie[1], Jayanti Pande[1]*, Ajay Pande[2], Jennifer A. Zarutskie[3] Joseph Lomakin[1], Aleksey Lomakin[1], Olutayo Ogun[1] Lawrence J. Stern[3], Jonathan King[2] and George B. Benedek[1]

[1]*Department of Physics*

[2]*Department of Biology Center for Materials Science and Engineering and Materials Processing Center Massachusetts Institute of Technology, Cambridge MA 02139-4307, USA*

[3]*Department of Chemistry*

**Corresponding author*

The cysteine residues of the γ crystallins, a family of ocular lens proteins, are involved in the aggregation and phase separation of these proteins. Both these phenomena are implicated in cataract formation. We have used bovine γB crystallin as a model system to study the role of the individual cysteine residues in the aggregation and phase separation of the γ crystallins. Here, we compare the thermodynamic and kinetic behavior of the recombinant wild-type protein (WT) and the Cys18 to Ser (C18S) mutant. We find that the solubilities of the two proteins are similar. The kinetics of crystallization, however, are different. The WT crystallizes slowly enough for the metastable liquid-liquid coexistence to be easily observed. C18S, on the other hand, crystallizes rapidly; the metastable coexisting liquid phases of the pure mutant do not form. Nevertheless, the coexistence curve of C18S can be determined provided that crystallization is kinetically suppressed. In this way we found that the coexistence curve coincides with that of the WT. Despite the difference in the kinetics of crystallization, the two proteins were found to have the same crystal forms and almost identical X-ray structures. Our results demonstrate that even conservative point mutations can bring about dramatic changes in the kinetics of crystallization. The implications of our findings for cataract formation and protein crystallization are discussed.

Keywords: γ crystallins; cataract; crystallization; X-ray structure; liquid-liquid coexistence

Bovine γB crystallin is a member of a highly homologous family of mammalian lens proteins known as the γ crystallins.[1] Together with the α and β crystallins, these proteins are essential for maintaining the proper refractive index gradient of the eye lens.[2] The γ crystallins differ from the α and β crystallins in two important respects. Firstly, the interactions between the γ crystallins are attractive.[3] The attractive interactions reduce the osmotic pressure in the lens, but they also makes the γ crystallins more susceptible to aggregation and phase separation, phenomena which diminish the homogeneity of the lens and lead to cataract.[4] Secondly, the γ crystallins contain a large number of cysteine residues. These residues are all in the reduced state and so free to react.[5] Indeed, modifications of the cysteine residues lead to the formation of high molecular weight aggregates in age-onset nuclear cataract.[6,"7] Yet, despite the potentially deleterious effects of the attractive interactions and the reactive cysteine residues, the γ crystallins remain soluble for many years at high concentrations and with little turnover, maintaining lens transparency.

In order to understand the role of the cysteine residues in the aggregation and phase separation of the γ crystallins, we have been studying native bovine γB crystallin as a model system. We have introduced conservative (Cys to Ser) point

Present address: J. Lomakin, Department of Chemical and Biological Engineering, Tufts University, Medford, MA 02155-6013, USA.

Abbreviations used: NA, native bovine γB crystallin isolated from young bovine lenses; WT, recombinant wild-type bovine γB crystallin expressed in *E. coli*; C18S, Cys18 to Ser mutant of WT; DTT, dithiothreitol.

E-mail address of the corresponding author: jpande@mit.edu

0022-2836/01/040663–7 $35.00/0

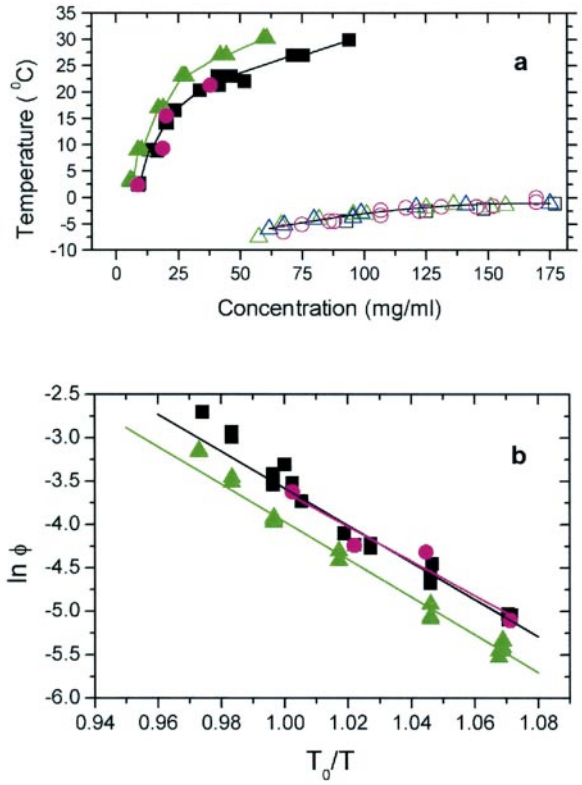

Figure 1. Phase diagram of WT, NA and C18S. (a) The solubility curves of WT (filled black squares), NA (filled magenta circles) and C18S (filled green triangles) are shown together with the liquid-liquid coexistence curves of WT (open black squares), NA (open magenta circles) and the 5% WT (open green triangles) and 10% WT (open blue triangles) mixtures with C18S. The lines are guides to the eye. (b) Log-linear plot of the solubility curves in Figure 1(a) used to extract the enthalpies and entropies of the protein crystals. The lines are fits to equation (1). T_0 is a reference temperature which was taken to be 295 K. Methods: Crystals were produced by quenching a high concentration (50-125 mg/ml) protein solution to −9 °C for five minutes to promote crystal nucleation. The solution was then brought back to room temperature where crystal growth occurred. This procedure separates the nucleation stage from that of growth and has been used to study nucleation kinetics in lysozyme.[17] To compare nucleation rates for different proteins, the initial concentrations were chosen so that at the quench temperature the supersaturations of the solutions were approximately the same. All solutions contained 0.1 M phosphate buffer (pH 7) with 20 mM DTT. This reducing agent was added to suppress thiol-mediated protein dimerization and subsequent aggregation, for these phenomena interfere with crystal formation. To determine the solubility curves, crystals were placed at a fixed temperature in fresh solutions of the phosphate buffer with DTT. As the crystals melted, the concentration of protein in solution was monitored by removing aliquots of the supernatant and measuring the absorbance at 280 nm. The system was deemed to be in equilibrium when the concentration of the solution reached a constant value. The solution-crystal system was continuously stirred to ensure thorough mixing of the components. The coexistence curves were determined by measuring the temperatures at which a protein solution of known concentration (and composition, in the case of mixtures) clouded upon cooling and cleared upon heating. The phase separation temperature was taken to be the average of the clouding and clearing temperatures. Details of this method are given in Liu *et al.*[18]

mutations at individual cysteine residues of this protein and have found that these mutations markedly affect the aggregation and phase behavior of the protein. Here, we compare the phase behavior of the Cys18 to Ser (C18S) mutant with that of the native bovine γB crystallin (NA) and the recombinant wild-type protein (WT). Our findings on the other mutants of bovine γB crystallin will be discussed elsewhere.

Phase behavior

A characteristic of solutions of the γ crystallins is that they exhibit two phase transitions: crystallization[8] and liquid-liquid phase separation.[9,10] Both transitions occur upon cooling. In crystallization,
a solid (crystal) forms from the protein solution. The solubility (at any given temperature) is the concentration at which the protein solution is in equilibrium with the crystal phase. In liquid-liquid phase separation, the solution separates into two coexisting liquid phases of unequal protein concentration. This liquid-liquid phase separation is brought about by the attractive interactions between the γ crystallins.[11] The coexistence curve is the locus of coexisting concentrations at various temperatures. Although liquid-liquid phase separation is metastable with respect to crystallization (i.e. it occurs at a lower temperature), crystal formation in the γ crystallins is usually slow enough so that the coexistence curve can still be measured.[10]

We determined the solubilities and the liquid-liquid coexistence curves for WT and C18S as well as for NA (Figure 1(a)). The solubilities of WT (filled black squares), NA (filled magenta circles) and C18S (filled green triangles) are all very similar. This is as expected, since WT and NA are the same protein, and the cysteine-to-serine substitution made in the mutant is conservative.

Unexpectedly, the mutant protein forms crystals much more quickly than the wild-type or native protein. C18S crystallizes in a matter of hours, while it takes days or even weeks for crystals of WT or NA to form. All three proteins form crystals of similar shape and size. The rapid crystallization of C18S is caused by an enhanced nucleation rate and not by a faster growth rate; when solutions of WT are seeded with WT crystals, crystal growth occurs at the same rate as in solutions of C18S seeded with C18S crystals. It is interesting to note that cross-seeding is not effective. Crystals do not grow in solutions of WT seeded with C18S crystals.

The slow crystallization allows the liquid-liquid coexistence curves of the WT (open black squares) and NA (open magenta circles) to be readily determined and they are identical. The rapid crystallization of C18S, however, renders a direct measurement of its coexistence curve impossible.

An indirect determination of the location of the C18S coexistence curve is possible if the crystallization of the protein is suppressed. We have found that in solutions of C18S which contain 5 % of WT (by number), the crystallization of C18S is delayed by approximately 24 hours as compared to pure solutions of C18S at the same total protein concentration. The crystals which do eventually form in this mixture consist of pure C18S. In solutions with 10 % of WT, crystallization is not observed at all. Since the WT and C18S proteins are similar, and the amounts of WT in the mixtures are small, the coexistence curve of the pure C18S can be calculated from the coexistence curves of the mixtures.[12] We found that the coexistence curves of C18S mixtures with 5 % (open green triangles) and 10 % (open blue triangles) of WT coincide with that of the pure WT protein (Figure 1(a)). From this we deduced that the coexistence curve of pure C18S coincides with that of WT. This result is not surprising given that liquid-liquid phase separation is mainly governed by the average energy of interaction between the proteins,[13] and the conservative mutation introduced should barely alter this average energy.

The enthalpies (ΔH) and entropies (ΔS) of crystal formation provide a quantitative measure of the similarity between the interactions of the proteins, for the enthalpy is related to the local energies of binding at the crystal contacts, while the entropy is a measure of the freedom lost upon crystallization.[14] These enthalpies and entropies may be extracted from the dilute region of the solubility curves using the van't Hoff equation:[15]

$$\ln \phi = \frac{\Delta H}{RT} - \frac{\Delta S}{R} \qquad (1)$$

Here, ϕ is the volume fraction of protein in solution. (It is related to the concentration C (in mg/ml) by the expression $\phi = \overline{v}C$, where $\overline{v}$ is the specific volume, which is taken to be 7.1×10^{-4} ml/mg.[10]), R is the universal gas constant, and T is the temperature. In Figure 1(b), we show the solubility curves of WT (black squares), NA (magenta circles) and C18S (green triangles) together with the fits to equation (1). Only the concentrations below 50 mg/ml, where the γ crystallins may be considered dilute,[11] were used in the fits. The deviations from the fits at higher concentrations are due to the attractive interactions between the proteins.[11,16] To within the experimental error, the enthalpies and entropies of crystal formation of WT, C18S and NA are identical (Table 1).

Why does C18S crystallize so much more rapidly than WT or NA? One possibility is that the mutant and wild-type proteins have different crystal forms. It is well known that different crystal forms nucleate at different rates.[19] This phenomenon has been investigated extensively for lysozyme.[20,21] We have observed it in human γD crystallin and a mutant (Arg36 to Ser),[22] which leads to a congenital cataract.[23] Although the secondary and tertiary structures of these two proteins are very similar, they have different unit cells (Kmoch *et al.*;[23] A. Basak & C. Slingsby, personal communication) and require different initial supersaturations for crystals to form (the supersaturation is defined as the ratio of the protein concentration in solution to the solubility).

We determined the space groups and unit cells of the C18S and WT crystals to check if they were the same. We also compared the X-ray structures of the two proteins to verify that the mutation had not significantly affected the three dimensional structure of the protein, and thus demonstrate that the altered kinetics were not due to a major conformational change in the protein.

Structure determination

The structure of C18S γB crystallin was determined using diffraction data collected with CuKα radiation and a single crystal at room temperature. Initial phase estimates were obtained by molecular replacement using the 1.47 Å model of the native γB crystallin[24] with the loop containing the mutation as well as residues above and below the mutation omitted. The initial electron-density maps were improved by cycles of manual model building and automated refinement. Unambiguous electron density was observed for the region containing the C18S mutation (Figure 2(a)).

The crystal forms of the C18S mutant and the native γB crystallin were very similar to each other. The C18S mutant had unit cell dimensions of $a = b = 57.85$ Å, $c = 98.71$ Å, and $\alpha = \beta =$

Table 1. Thermodynamic parameters for the crystallization of WT, NA and C18S

Protein	C_{eq} (T_0) (mg/ml)	$\Delta G(T_0)$ (kJ mol^{-1})	ΔH (kJ mol^{-1})	$-T_0\Delta S$ (kJ mol^{-1})
WT	39.3	−8.8	−52.4	43.6
NA	37.7	−8.9	−48.9	40.0
C18S	26.6	−9.7	−53.2	43.5

$C_{eq}(T_0)$ is the solubility at T_0 (a reference temperature which was taken to be 295 K). ΔG, ΔH and ΔS are, respectively, the Gibbs free energy ($\Delta G = \Delta H - T\Delta S$), the enthalpy and the entropy of formation of the crystal phase for each protein.

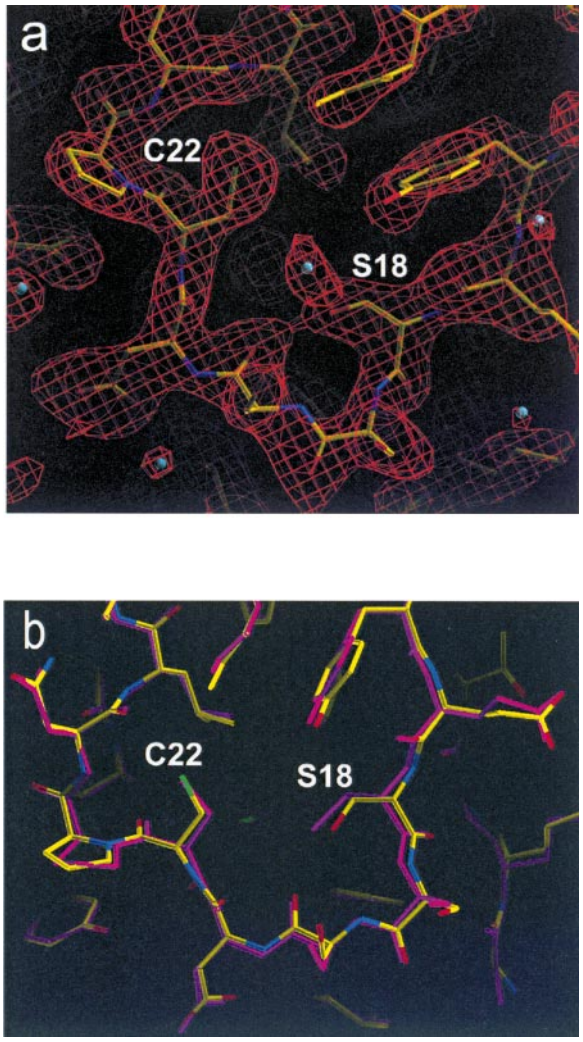

Figure 2. (a) Loop electron density for C18S. Map calculated with $|2F_o - F_c|$ coefficients and model phases, contoured at 1σ, using the final refined model. The bonds in the model are colored according to atom type (red, oxygen; blue, nitrogen; yellow, carbon; and green, sulfur). Water molecules are shown as cyan spheres. The positions of Ser18 and Cys22 are indicated above the residues. (b) Comparison of loop conformation between the C18S mutant and native γB crystallin structures. The residues of the reduced native γB crystallin structure[24] are in magenta, and the residues of the C18S mutant are as described in (a). The conformations of the two loops are similar, with an average rms deviation of 0.18 Å between the main-chain coordinates and an average rms deviation of 0.39 Å between the side-chain coordinates. Methods: A single crystal (1 mm × 0.4 mm × 0.1 mm) was harvested into 100 mM sodium phosphate pH 7.0 + 1 mM DTT. The crystal was mounted in a 1 mm diameter quartz capillary tube and maintained at room temperature (23 °C) throughout the data collection. Diffraction data were collected using CuKα radiation (λ = 1.5418 Å) generated using a Rigaku RU200 rotating copper anode source. The data were recorded at a distance of 120 mm on RAXIS II image plates at an exposure time of 15 minutes. An oscillation angle of 1 ° per image was used. Diffraction intensities were integrated and scaled using DENZO and SCALEPACK.[26] An overall isotropic *B*-factor was estimated to be 28 Å from a Wilson plot, with no evidence of anisotropy. Initial phases were determined by molecular replacement using AmoRE,[27] with a 1.47 Å structure of bovine γB crystallin[24] as the search model. This model comprised one native γB crystallin with residues Lys2 to Phe5, His14 to Ser30, Tyr42, and Cys78 to Leu80 removed. A rotation search using 10-3.5 Å data revealed one unique solution. Electron-density maps calculated omitting subsections of the model revealed clear density for the omitted regions. A model for the omitted regions was built and the initial model was adjusted using averaged electron-density maps that were calculated by omitting coordinates for the region under consideration. The rebuilt model was refined using X-PLOR[28] with rigid body, simulated annealing, positional and restrained *B*-factor refinement steps. After nine cycles of rebuilding and refinement the *R*-factor was 0.223 and the free R-factor was 0.243. Water molecules were added based on peaks in $F_{obs} - F_{calc}$ difference maps identified using the CCP4 suite of programs[29] and SHELX,[30] and on hydrogen-bonding distance and geometry criteria. Refinement steps using SHELX[30] were included in cycles six, seven, and eight. The final model includes coordinates for 173 residues (1458 protein atoms) and 71 water molecules. Weak to non-existent electron density was observed for Met160 C^{ε}, C^{γ} and S, and thus those atoms were not included in the residue. The C-terminal Tyr174 was also omitted from the model for the same reason. Model geometry was examined using PROCHECK[25] and was found to meet or exceed criteria determined for the 1.47 Å structure of bovine γB crystallin.[24] No residues fell outside the allowed regions of a Ramachandran plot. Average cross-validated coordinate error was estimated to be 0.27 Å by Luzzati analysis[31] and 0.19 Å by SIGMAA analysis.[32]

$\gamma = 90^\circ$ in space group $P4_12_12$ (Table 2) with one protein in the asymmetric unit, while NA had unit cell dimensions $a = b = 57.53$ Å, $c = 97.95$ Å, and $\alpha = \beta = \gamma = 90^\circ$ in the same space group with one protein in the asymmetric unit as well.[24] Comparison of the refined structure of C18S with that of the reduced NA revealed that the overall conformation of the proteins was essentially identical, as was the loop region containing the C18S mutation (Figure 2(b)). For the residues in the loop, an average rms deviation of 0.18 Å between the main-chain coordinates and an average rms deviation of 0.39 Å between the side-chain coordinates was calculated. The pattern of hydrogen bonds among the residues in the loop were similar, except that Ser18 in the mutant makes two additional hydrogen bonds, one to the backbone carbonyl group of Ser20 and the other to a nearby water molecule that was not observed in the native structure (Figure 2(a)). It is possible that the modification in hydrogen bonding brought about by the mutation is involved in the enhanced nucleation of C18S. If this is the case, it is unclear why the mutation only affects the crystal nucleation rate, but not any of the fundamental thermodynamic parameters. However, since the mutation has little effect on the structure of the γB crystallin protein, the enhanced

Table 2. Data collection and refinement statistics

A. *Cell parameters (space group $P4_12_12$)*	
$a = b$ (Å)	57.85
c (Å)	98.71
$\alpha = \beta = \gamma$ (deg.)	90.00
B. *Data collection*	
Wavelength, (Å)	1.5418
Resolution (Å)	30.0-2.4 (2.44-2.40)[a]
Mosaicity (deg.)	0.3
Total no. reflections	68,447
No. unique reflections	6843
Completeness (%)	97.1 (92.8)[a]
Average $I/\sigma I$	21.6 (9.6)[a]
R_{merge} (%)[b]	7.4 (14.6)[a]
C. *Refinement (20.0-2.4 Å)*	
No. reflections (free)	5998 (679)
R_{cryst} (%)[c]	22.3
R_{free} (%)[d]	24.3
Average B (Å^2), overall	13.2
Average B (Å^2), protein	11.9
Average B (Å^2), water	37.9
rmsd bonds (Å)	0.009
rmsd angles (deg.)	1.21
rmsd dihedrals (deg.)	28.6
Ramachandran Plot[e]	
Favored (%)	88.7
Allowed (%)	11.3

[a] Numbers in parenthesis denote values in the highest resolution shell.
[b] R-factor $(\Sigma|I(hkl) - \langle I\rangle|/\Sigma I)$ on intensity for symmetry-related reflections.
[c] R-factor $(\Sigma|F_{obs} - F_{calc}|/F_{obs})$ on structure factors for reflections used in refinement (90 % of total).
[d] R-factor on structure factors for reflections omitted at random from the refinement and used as a test set (10 % of total).
[e] As defined in PROCHECK.[25]

nucleation is not caused by any significant conformational change.

Discussion and conclusion

Loss of solubility in the γ crystallins is associated with lens opacity.[33] Point mutations which enhance protein crystallization, such as the one we have studied here, can lead to cataract formation. Indeed, we have recently shown that two human genetic cataracts are caused by the enhanced crystallization of mutant γD crystallins.[22] In the case of the Arg36 to Ser mutation of human γD crystallin, crystals of the mutant protein have been in fact isolated from the lens of a young patient.[23]

Several instances of amino acid substitutions leading to increased crystal nucleation rates have been reported. The rationales included strengthening or introducing a crystal contact,[34] constructing the building blocks of the crystal (e.g. forming dimers out of a monomeric protein for which it is known that the asymmetric unit in the crystal is a dimer)[35] and suppressing aggregation by removing a reactive residue, generally a cysteine residue.[36] None of these rationales explain the enhanced nucleation of the C18S mutant. The Cys18 residue is not at a crystal contact and the asymmetric unit of the crystal is a monomer. Furthermore, the enhanced nucleation was observed under reducing conditions; the solutions of WT and C18S remained essentially monomeric over the course of the crystallization experiments.

The inability of C18S and WT to co-crystallize is also intriguing. Proteins which are as similar as C18S and WT generally co-crystallize,[37] and co-crystallization has been reported for pairs of proteins which are fairly different in structure.[19] It is also surprising that C18S did not act as a seed for WT. Cross-seeding of proteins is usually successful with similar proteins[38] and often works with proteins which do not resemble each other as much as C18S and WT do.[39]

The absence of co-crystallization suggests that in the mixtures it is the C18S alone that is involved in crystal nucleation. Nevertheless, the observed reduction in nucleation rate found in the mixtures is much more than expected from classical nucleation theory. According to this theory, the nucleation rate is proportional to the probability of producing a critical nucleus of n proteins.[40,41] This probability contains a factor of c^n, where c is the concentration in solution of the nucleating species. The presence of inert WT in the mixtures simply reduces c by dilution. According to this picture, the observed halving of the nucleation rate in the 5 % mixture (as compared to pure C18S) implies that $n = \ln(1/2)/\ln(0.95) \approx 14$. Although this is a reasonable size for a critical nucleus of a protein crystal,[42,43] this value of n implies that for the 10 % mixture, there should be only about a fourfold reduction in nucleation rate. The actual nucleation rate dropped by more than 14-fold. This discrepancy illustrates the limitations of classical nucleation theory when applied to protein solutions.[17]

Our work shows that even a conservative point mutation in a protein can produce an order of magnitude increase in the rate of crystallization. This increase occurred without any change in the solubility of the protein, the crystal form, or the protein conformation in the crystal. According to conventional criteria, the enhanced nucleation of C18S crystals should involve one or more of the following factors: a crystal contact, the formation of the asymmetric unit, or the suppression of aggregation. Our data shows that the increase in the rate of crystallization of C18S does not involve any of these factors. Unraveling the mechanism underlying the enhancement of nucleation in C18S may prove valuable in the crystallization of other proteins.

Protein Data Bank accession code

Coordinates and structure-factor amplitudes have been deposited in the RCSB Protein Data Bank with accession code #1I5I.

Acknowledgments

We thank Dr Eva Mayr for the gift of the bovine γB crystallin cDNA clone, Dr Scott Betts for assistance with the initial phase of the mutagenesis work, Christina Collins for aid in initial model building and refinement and Dr Catherine Drennan, Dr. Tzanko Doukov and Mike Sintchak for aid and advice in all stages of the data processing and model building and refinement. This work was supported by the National Institutes of Health (U.S.A.) grants EY10535 to J.P., GM56552 to L.J.S, GM17980 to J.K., EY05127 to G.B.B., and a Merck-MIT collaboration graduate fellowship to J.A.Z.

References

1. Lindley, P. F., Narebor, M. E., Summers, L. J. & Wistow, G. J. (1985). The structure of lens proteins. In *The Ocular Lens: Structure, Function and Pathology* (Maisel, H., ed.), chapt. 4, pp. 123-167, Marcel Dekker, New York.
2. Zigler, J. S., Jr (1994). Lens proteins. In *Principles and Practice of Ophthalmology* (Alberts, E. M. & Jacobiec, F. A., eds), chapt. 6, pp. 97-113, W.B. Saunders, Philadelphia.
3. Tardieu, A., Vérétout, F., Krop, B. & Slingsby, C. (1992). Protein interactions in the calf eye lens: interactions between β-crystallins are repulsive whereas in γ-crystallins they are attractive. *Eur. Biophys. J.* **21**, 1-21.
4. Clark, J. I. (1994). Development and maintenance of lens transparency. In *Principles and Practice of Ophthalmology* (Alberts, E. M. & Jacobiec, F. A., eds), chapt. 7, pp. 114-123, W.B. Saunders, Philadelphia.
5. Norledge, B. V., Hay, R. E., Bateman, O. A., Slingsby, C. & Driessen, H. P. C. (1997). Towards a molecular understanding of phase separation in the lens: a comparison of the X-ray structures of two high T_c γ-crystallins, γE and γF, with two low T_c γ-crystallins, γB and γD. *Exp. Eye Res.* **65**, 609-630.
6. Jaffe, N. S. & Horwitz, J. (1992). Lens and cataract. In *Textbook of Ophthalmology* (Podos, S. M. & Yanoff, M., eds), vol. chap. 7, Gower, New York.
7. Harding, J. J. & Crabbe, M. J. C. (1984). The lens: development, proteins, metabolism and cataract. In *The Eye* (Davson, H., ed.), vol 1b, chapt. 3, pp. 435-439, Academic Press, New York.
8. Berland, C. R., Thurston, G. M., Kondo, M., Broide, M. L., Pande, J., Ogun, O. & Benedek, G. B. (1992). Solid-liquid phase boundaries of lens protein solutions. *Proc. Natl Acad. Sci. USA,* **89**, 1214-1218.
9. Thomson, J. A., Schurtenberger, P., Thurston, G. M. & Benedek, G. B. (1987). Binary liquid phase separation and critical phenomena in protein/water solution. *Proc. Natl Acad. Sci. USA,* **84**, 7079-7083.
10. Broide, M. L., Berland, C. R., Pande, J. *et al.* (1991). Binary-liquid phase separation of lens protein solutions. *Proc. Natl Acad. Sci. USA,* **88**, 5660-5664.
11. Lomakin, A., Asherie, N. & Benedek, G. B. (1996). Monte Carlo study of phase separation in aqueous protein solutions. *J. Chem. Phys.* **104**, 1646-1656.
12. Liu, C., Lomakin, A., Thurston, G. M., Hayden, D., Pande, A., Pande, J., Ogun, O., Asherie, N. & Benedek, G. B. (1995). Phase separation in multicomponent aqueous-protein solutions. *J. Phys. Chem.* **99**, 454-461.
13. Lomakin, A., Asherie, N. & Benedek, G. B. (1999). Aeolotopic interactions of globular proteins. *Proc. Natl Acad. Sci. USA,* **96**, 9465-9468.
14. Yau, S.-T., Petsev, D. N., Thomas, B. R. & Vekilov, P. G. (2000). Molecular-level thermodynamic and kinetic parameters for the self-assembly of apoferritin molecules into crystals. *J. Mol. Biol.* **303**, 667-678.
15. van Holde, K. E. (1985). *Physical Biochemistry*, 2nd edit., chapt. 3, pp. 56-57, Prentice-Hall, Englewood Cliffs.
16. Tanford, C. (1961). *Physical Chemistry of Macromolecules*, chap. 4, John Wiley & Sons, New York.
17. Galkin, O. & Vekilov, P. G. (1999). Direct determination of the nucleation rates of protein crystals. *J. Phys. Chem. sect. B,* **103**, 10965-10971.
18. Liu, C., Asherie, N., Lomakin, A., Pande, J., Ogun, O. & Benedek, G. B. (1996). Phase separation in aqueous solutions of lens γ-crystallins: special role of γS. *Proc. Natl Acad. Sci. USA,* **93**, 377-382.
19. McPherson, A. (1999)). *Crystallization of Biological Macromolecules*, Cold Spring Harbor Laboratory Press, Cold Spring Harbor NY.
20. Zhang, X.-J., Wozniak, J. A. & Matthews, B. W. (1995). Protein flexibility and adaptability seen in 25 crystal forms of T4 lysozyme. *J. Mol. Biol.* **250**, 527-552.
21. Ewing, F., Forsythe, E. & Pusey, M. (1994). Orthorhombic lysozyme solubility. *Acta Crystallog. sect. D,* **50**, 424-428.
22. Pande, A., Pande, J., Asherie, N., Lomakin, A., Ogun, O., King, J. & Benedek, G. B. (2001). Crystal cataracts: human genetic cataract due to protein crystallization. *Proc. Natl Acad. Sci. USA,* **98**, 6116-6120.
23. Kmoch, S., Brynda, J., Befekadu, A., Bezouška, K., Novák, P., Rezácová, P. *et al.* (2000). Link between a novel human γD-crystallin allele and a unique cataract phenotype explained by protein crystallography. *Hum. Mol. Genet.* **9**, 1779-1786.
24. Najmudin, S., Nalini, V., Dreissen, H. P. C., Slingsby, C., Bundell, T. L., Moss, D. S. & Lindley, P. F. (1993). Structure of the bovine lens protein γB (γII)-crystallin at 1.47 Å. *Acta Crystallog. sect. D,* **49**, 223-233.
25. Laskowski, R. A., MacArthur, M. W., Moss, D. S. & Thornton, J. M. (1993). PROCHECK: a program to check the stereochemical quality of protein structures. *J. Appl. Crystallog.* **26**, 283-291.
26. Minor, W. & Otwinoski, Z. (1997). Processing of X-ray diffraction data collected in oscillation mode. *Methods Enzymol.* **276**, 307-326.
27. Navazza, J. (1994). AmoRE: an automated package for molecular replacement. *Acta Crystallog. sect. A,* **50**, 157-163.
28. Brünger, A. T. (1992). *X-PLOR Version 3.1 Manual: A System for X-ray Crystallography and NMR*, Yale University Press, New Haven CT.
29. Collaborative Computational Project No. 4 (1994). The CCP4 Suite: programs for protein crystallography. *Acta Crystallog. sect. D,* **50**, 760-763.
30. Sheldrick, G. & Schneider, T. R. (1997). SHELX: high-resolution refinement. *Methods Enzymol.* **277**, 319-343.
31. Luzzati, V. (1952). Traitement statistique des erreurs dans la determination des structures cristalines. *Acta Crystallog.* **5**, 802-810.
32. Read, R. J. (1986). Improved Fourier coefficients for maps using phases from partial structures with errors. *Acta Crystallog. sect. A,* **42**, 140-149.

33. Benedek, G. B. (1997). Cataract as a protein condensation disease. *Invest. Ophthalmol. Vis. Sci.* **38**, 1911-1921.
34. Mittl, P. R. E., Berry, A., Scrutton, N. S., Perham, R. N. & Schulz, G. E. (1994). A designed mutant of the enzyme glutathione reductase shortens the crystallization time by a factor of forty. *Acta Crystallog. sect. D,* **50**, 228-231.
35. Heinz, D. W. & Matthews, B. W. (1994). Rapid crystallization of T4 lysozyme by intermolecular disulfide cross-linking. *Protein Eng.* **7**, 301-307.
36. Stover, C., Mayhew, M. P., Holden, M. J., Howard, A. & Gallagher, D. T. (2000). Crystallization and 1.1-Å diffraction of chorismate lyase from *Escherichia coli*. *J. Struct. Biol.* **129**, 96-99.
37. Treece, J. M., Shinson, R. S. & McMeekin, T. L. (1964). The solubilities of β-lactoglobulins A, B, and AB. *Arch. Biochem. Biophys.* **108**, 99-108.
38. Sanishvili, R. G., Margoliash, E., Westbrook, M. L., Westbrook, E. M. & Volz, K. W. (1994). Crystallization of wild-type and mutant ferricytochromes c at low ionic strength: seeding technique and X-ray diffraction analysis. *Acta Crystallog. sect. D,* **50**, 687-694.
39. Eichele, G., Ford, G. C. & Jansonius, J. N. (1979). Crystallization of pig mitochondrial aspartate aminotransferase by seeding with crystals of the chicken mitochondrial isoenzyme. *J. Mol. Biol.* **135**, 513-516.
40. Kashchiev, D. (1982). On the relation between nucleation work, nucleus size, and nucleation rate. *J. Chem. Phys.* **76**, 5098-5102.
41. Oxtoby, D. W. & Kashchiev, D. (1994). A general relation between nucleation work and the size of the nucleus in multicomponent nucleation. *J. Chem. Phys.* **100**, 7665-7671.
42. Galkin, O. & Vekilov, P. G. (2000). Are nucleation kinetics of protein crystals similar to those of liquid droplets?. *J. Am. Chem. Soc.* **122**, 156-163.
43. Yau, S.-T. & Vekilov, P. G. (2000). Quasi-planar nucleus structure in apoferritin crystallization. *Nature,* **406**, 494-497.

Edited by W. Baumeister

(Received 6 July 2001; received in revised form 27 September 2001; accepted 2 October 2001)